



Aalborg Universitet

AALBORG UNIVERSITY  
DENMARK

## **Hierarchical control of a photovoltaic/battery based DC microgrid including electric vehicle wireless charging station**

Xiao, Zhao xia; Fan, Haodong; Guerrero, Josep M.; Fang, Hongwei

*Published in:*

Proceedings of 43rd Annual Conference of the IEEE Industrial Electronics Society, IECON 2017

*DOI (link to publication from Publisher):*

[10.1109/IECON.2017.8216424](https://doi.org/10.1109/IECON.2017.8216424)

*Publication date:*

2017

*Document Version*

Early version, also known as pre-print

[Link to publication from Aalborg University](#)

*Citation for published version (APA):*

Xiao, Z. X., Fan, H., Guerrero, J. M., & Fang, H. (2017). Hierarchical control of a photovoltaic/battery based DC microgrid including electric vehicle wireless charging station. In *Proceedings of 43rd Annual Conference of the IEEE Industrial Electronics Society, IECON 2017* (pp. 2522-2527). IEEE Press.  
<https://doi.org/10.1109/IECON.2017.8216424>

### **General rights**

Copyright and moral rights for the publications made accessible in the public portal are retained by the authors and/or other copyright owners and it is a condition of accessing publications that users recognise and abide by the legal requirements associated with these rights.

- Users may download and print one copy of any publication from the public portal for the purpose of private study or research.
- You may not further distribute the material or use it for any profit-making activity or commercial gain
- You may freely distribute the URL identifying the publication in the public portal -

### **Take down policy**

If you believe that this document breaches copyright please contact us at [vbn@aub.aau.dk](mailto:vbn@aub.aau.dk) providing details, and we will remove access to the work immediately and investigate your claim.

# Hierarchical Control of a Photovoltaic/Battery based DC Microgrid Including Electric Vehicle Wireless Charging Station

Xiao Zhaoxia<sup>1</sup>, Fan Haodong<sup>1</sup>, Josep M. Guerrero<sup>2</sup>

1. Tianjin Key Laboratory of Advanced Technology of Electrical Engineering and Energy  
Tianjin Polytechnic University, P. R. China, Email: xiaozhaoxia@tjpu.edu.cn

2. Department of Energy Technology, Aalborg University, Denmark, [joz@et.aau.dk](mailto:joz@et.aau.dk), [www.microgrids.et.aau.dk](http://www.microgrids.et.aau.dk)

**Abstract**—In this paper, the hierarchical control strategy of a photovoltaic/battery based dc microgrid is presented for electric vehicle (EV) wireless charging. Considering irradiance variations, battery charging/discharging requirements, wireless power transmission characteristics, and onboard battery charging power change and other factors, the possible operation states are obtained. A hierarchical control strategy is established, which includes central and local controllers. The central controller is responsible for the selection and transfer of operation states and the management of the local controllers. Local controllers implement these functions, which include PV maximum power point tracking (MPPT) algorithm, battery charging/discharging control, voltage control of DC bus for high-frequency inverter, and onboard battery charging control. By optimizing and matching parameters of transmitting coils, receiving coils and compensation capacitors, the wireless power transmission system is designed to be resonant when it is operating at the rated power, with the aim to achieve the optimum transmission system efficiency. Simulation and experimental results of the hierarchical control of the microgrid with electric vehicle wireless charging are established, showing the effectiveness of the proposed approach.

**Keywords**—DC microgrid; EV wireless charging; hierarchical control; operation states; magnetic resonance coupling

## I. INTRODUCTION

The randomness and intermittence of large number of EVs charging will put forward new requirements and challenges to the traditional power grid and charging facilities [1]-[2]. Microgrid is an important way to increase the reliability of power supply, while enhancing the quality of users' electricity consumption, and to improve the efficiency of distributed power supply and the user side safety of the consumption capacity of renewable energy [3-6]. Wireless power transmission (WPT) uses non-contact transmission of energy to make up for the shortcomings of traditional direct contact power supply, and at the same time can increase the flexibility and security of power supply, becoming an effective way of EVs charging. The microgrid technology and WPT applied to

EVs charging and integrated into a whole system through the microgrid may become one effective method to solve onsite the EVs charging. This method can effectively reduce the traditional power grid upgrading requirements and the impact of high-power short-term charging of the traditional power grid. It also may solve the construction of various types of charging piles, decentralized electric vehicle charging concentration and increase the flexibility of charging. Also through the control and management of the microgrid can provide higher quality electricity for EV.

At present, research on microgrids for EVs charging mainly includes: control strategies, economic analysis, power flow calculation, vehicle battery to participate in the microgrid operation, and so on [7]-[10]. There are three kinds of transmission modes of WPT: electromagnetic induction, magnetic coupling resonance and microwave radiation [11]. The current research on WPT and EVs wireless charging mainly includes: the design of resonant transceiver coil structure and the control and management of vehicle battery.

This paper studies the hierarchical control strategy of DC microgrids for EVs wireless charging, including design of the local controllers of microgrids, design of the wireless charging side voltage controller, and design of the energy management system.

The structure of this paper is as follows. Section II introduces the structure of the hierarchical control system of the DC microgrid with EVs wireless charging. Section III analyzes the possible operating modes of the system and the operating status of the PV panels and the battery pack. In Section IV, the structure of the controller is introduced, including the battery charging/discharging controller, the DC bus voltage controller of the high frequency (HF) inverter side and the charging controller of the vehicle battery and the wireless charging system. The wireless charging system is in resonance state by optimizing the matching transceiver inductor and the compensation capacitor parameters. Sections V and VI shows the simulation and experimental results. Section VII gives the conclusion of the paper.

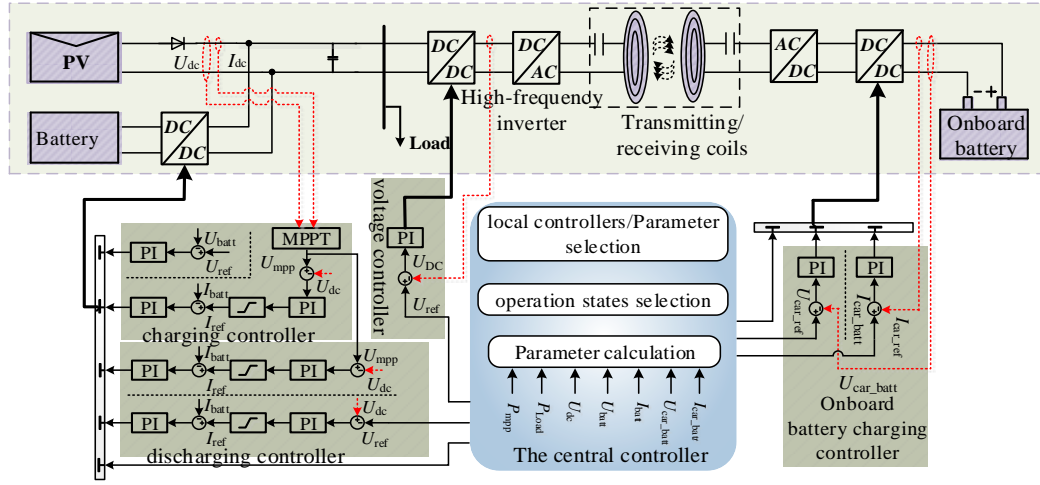


Fig. 1. Hierarchical control of PV/battery microgrid with EV wireless charging.

## II. HIERARCHICAL CONTROL FOR PV MICROGRID WITH EV WIRELESS CHARGING

The structure of the hierarchical control of a PV microgrid with electric vehicle wireless charging is shown in Fig. 1. The first part of the system is composed of a PV based microgrid, wireless charging system, load, and battery. The PV based microgrid comprises a PV power generating unit, a DC/DC converter and a battery unit. The PV unit and the battery unit, which is controlled by a bidirectional DC/DC converter, are connected in parallel to the DC bus. The wireless charging system comprises a DC/DC converter, a DC/AC HF inverter, a receiving/transmitting coil and a corresponding tuning capacitor. The electric energy generated by PV microgrid is converted to 20 kHz HF voltage by DC/DC converter and DC/AC HF inverter for the wireless transmitter power supply. The resonant system can efficiently transmit power by the transmitting coils to the load power supply. The vehicle battery system comprises an AC/DC rectifier, a DC/DC converter, and a vehicle battery.

The second part of the control system mainly includes central and the local controllers. The central controller is mainly used to assess the operation mode of the system, select the local controller, and set the parameters. The local controller comprises a battery charging/discharging controller, a HF inverter DC bus voltage controller, and a vehicle battery charging controller. Under the coordination of the upper central controller and the local controller, the PV microgrid can provide stable and efficient electric energy for EV charging through the wireless charging system.

### III. CENTRAL CONTROLLER

Considering the variations of the PV power with the illumination intensity, the relationship between the PV power and the load power is found as shown in Fig. 2. According to the relationship between photovoltaic power and load power, the photovoltaic microgrid for the electric vehicle wireless charging system operating mode as shown in Fig. 2.

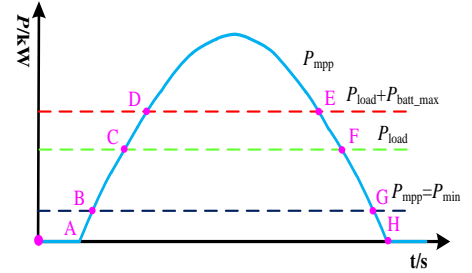


Fig. 2. Relationship between PV maximum power and load power.

According to Fig. 3, the operating conditions of the system are as follows:

- (1) AB segment. The illumination intensity is weak, the maximum power of photovoltaic power  $P_{mpp} < P_{min}$  (The simulation system sets the PV starting power  $P_{min} = 10kW$ ), the PV is off and the battery discharge alone to maintain a constant DC bus voltage. The battery side DC/DC converter controller is a constant voltage controller and the system is running in mode I. When the remaining capacity of the battery is less than the minimum remaining capacity or the battery voltage is less than the minimum discharge voltage, the battery stops discharging and the system is shut down and run in mode VI.
- (2) BC segment. Increase of illumination intensity, the maximum power of photovoltaic power generation  $P_{mpp} \geq P_{min}$ , but  $P_{mpp} < P_{Load}$ , ( $P_{Load}$  is the total load power). The battery discharging controller contains the DC bus voltage  $U_{dc} = U_{mpp}$  ( $U_{mpp}$  is the photovoltaic voltage at which the maximum power is output for photovoltaic). The battery side DC / DC controller is the maximum power point tracking (MPPT) controller for discharge, at this time the system runs in mode II. If the battery is empty, the system shuts down and runs in mode VI.
- (3) CD Segment. The maximum photovoltaic power generation  $P_{mpp} \geq P_{Load}$  and  $P_{mpp} < P_{Load} + P_{batt\_max}$  ( $P_{batt\_max}$  is the maximum charging power of the battery), PV in the maximum power tracking state for the load power supply while charging the battery. The battery side DC/DC controller is the maximum power tracking controller for charging at this time the system runs in mode III.

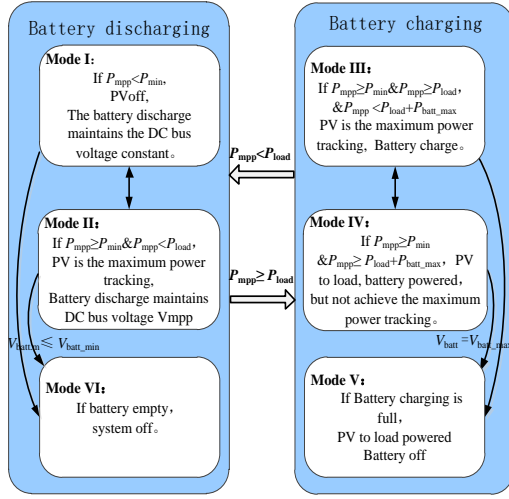


Fig. 3. Switches of system operation modes.

(4) DE segment. The maximum photovoltaic power generation  $P_{mpp} \geq P_{load} + P_{batt\_max}$ , the PV exits the maximum power running and charging the battery while supplying for the load. Battery select constant current or constant voltage charging according to the state of charging, the system runs in mode IV.

(5) In the EF segment, the operating conditions of the system are the same as (3).

(6) In the FG segment, the operating conditions of the system are the same as (2).

(7) In the GH segment, the operating conditions of the system are the same as (1).

In view of the above seven modes of operation, this paper uses *Matlab/Stateflow* to design the upper center controller to realize the system energy management and running state transition to ensure the reliable charging of EVs.

#### IV. LOCAL CONTROLLER

##### A. Common DC bus control

The PV array is directly connected to the DC bus and the DC bus voltage. The output power-voltage characteristic curve of photovoltaic panel under different illumination conditions can change considerably.

When this occurs, the stable operation of the PV system is located in the right side of the maximum power point [17]. The output voltage of the PV DC voltage determines its output power. By controlling the PV array to work in the maximum power point, we can control the DC bus voltage, and then achieve the maximum power output of the PV array.

##### B. Design of battery side DC / DC controller

###### 1) Battery discharge controller

When the system operates in modes I and II, the battery is in discharging state, and the battery side DC/DC controller is shown in Fig. 4. The outer loop of the controller is a voltage one and the inner loop is a current one. The voltage loop includes a constant voltage control loop and an MPPT loop. Current loop ensure the discharge current does not exceed the limit. The output voltage loop of the PI signal is used as the

reference value of the discharge current of the current loop, and the reference value of the maximum discharge current is 150A in this case.

When the system is operating in mode I, the constant voltage control loop is used to maintain the DC bus voltage at 500V. When the system is operating in mode II using the MPPT loop is used to achieve battery discharge and keep the DC bus voltage in the PV MPPT voltage  $U_{mpp}$ . The current inner loop prevents the battery discharge current from exceeding the limit value.

###### 2) Battery charging controller

When the system is operating in mode III and mode IV, the battery is in charge and charging control, is shown in Fig. 5. The charge controller uses also a double closed-loop control. When the maximum power tracking of the PV is realized, the PI output signal is used as the reference value of the internal loop current charging current, see Fig. 5 (a).

Here, the reference value of the maximum charge current is 60A. When the actual charging current of the battery reaches the limit amplitude, the system transits from the operating mode III to IV. With the increase of battery power, the state of charge (SOC) will change and the battery port voltage will rise. When the battery port voltage reached 95%, it will transfer to constant voltage charging control, see Fig. 5(b). When the battery voltage reaches its maximum value and the charging current is less than its minimum value, the battery is fully charged and the charging process is stopped.

##### C. Parameter Selection and Controller Design of Resonant Wireless Charging

The wireless charging system is shown in Fig. 6. It mainly includes HF inverter side of the DC bus constant voltage control DC/DC converter, a DC/AC HF inverter, a transceiver coil and a compensation capacitor, an AC/DC rectifier, a DC/DC converter for vehicle battery charging, and an electric vehicle battery.

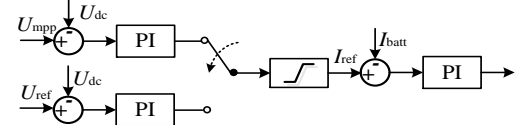


Fig. 4. Discharge controller.

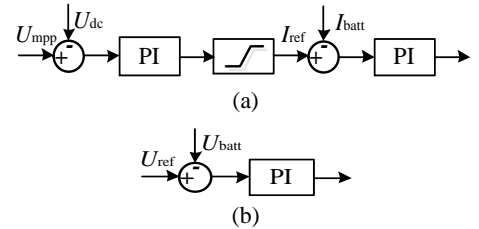


Fig. 5. Charge controllers: (a) constant current and (b) constant voltage.

Due to fluctuations of PV power generation, the voltage of the PV side is constantly changing. If the HF inverter is directly connected to the DC bus of the PV side, the system is difficult to control when the power demand of the vehicle

battery changes, and the control complexity of the HF inverter is relatively large. Therefore, this paper first optimizes the parameters of the resonant wireless charging system, so that the system is in the resonant state when it is running at rated power. Then, the DC/DC converter is added in front of the HF inverter to control the wireless charging system.

In order to improve the energy transfer efficiency of the wireless charging system, and to make the system operate in the resonant state, the string compensation (SS) topology is selected to optimize the system transceiver loop, see Fig. 6; where  $\omega$  is the angular frequency,  $M$  is the mutual inductance of the transceiver coil,  $L_s$  and  $L_r$  are the transmitter and receiver coil ( $s$  stands for transmitter and  $r$  stands for receiver);  $C_s$  and  $C_r$  are the added string compensation (SS) capacitors;  $z_L$  is the equivalent impedance of the car battery at rated frequency;  $U_{in}$  is the input voltage of the transmitter coil; and  $i_s$  and  $i_r$  are the current values of the transmitter and the receiver. The resistance value of the transmitter and receiver coils at the rated angular frequency are negligible respect to the inductance and capacitive resistance in the system circuit, so that they are not considered.

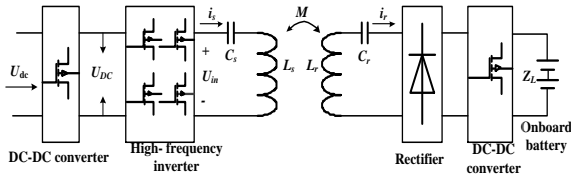


Fig. 6. Wireless charging system.

The impedance values  $z_s$ ,  $z_r$  and  $z_L$  of the transmitting coil, the receiving coil and the load are as follows:

$$Z_s = j\omega L_s + 1/j\omega C_s \quad (1)$$

$$Z_r = j\omega L_r + 1/j\omega C_r + Z_L \quad (2)$$

$$Z_L = R_L + jX_L \quad (3)$$

When the transmitter and the receiver coils are coupled, by ignoring the impedance of the receiver converter, the equivalent impedance  $z_{sr}$ :  $Z_{sr} = (\omega M)^2 / Z_r$ . So that the total equivalent impedance of the *transmitter* loop is  $Z_{eq} = Z_s + Z_{sr}$ .

By ignoring switching losses,  $U_{in}$  is approximately equal to the effective value of the  $U_{DC}$ ,

$$U_{in} \approx 2\sqrt{2}U_{DC} / \pi \quad (4)$$

The power of the system from the transmitter to the receiver coils, that is, the power of the load, can be expressed as

$$P_L = U_{in}^2 / \text{Re}(Z_{sr}) \quad (5)$$

being  $\text{Re}(Z_{sr})$  the impedance real part of the receiver circuit coupled to the transmitter circuit. When the system is in the resonance state,  $z_r$  obtains the minimum value, and  $z_{sr}$  gets the maximum value. When the system is in resonance state,  $z_r$  obtains the minimum value and  $z_{sr}$  gets the maximum value,  $Z_{sr} = (\omega M)^2 / R_L$ , then the load power can be expressed as:

$$P_L \approx 8U_{DC}^2 R_L / \pi^2 \omega^2 M^2 \quad (6)$$

The corresponding controller is shown in Fig. 7, which is a voltage controller. The input voltage of HF inverter is deduced by the above formula and this voltage is used as the reference value of the DC/DC voltage controller of the DC bus voltage side of the HF inverter.

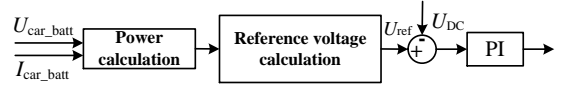


Fig. 7. Constant voltage controller.

## V. SIMULATION RESULTS

In this paper, we use *Matlab/Simulink* software to simulate the PV based microgrid with EV wireless charging shown in Fig. 1. The PV based microgrid consists of a battery of 192 series-connected cells, with a total capacity of 800Ah and a rated voltage of 384V, an EV battery capacity of 50Ah, and rated voltage of 266V. The main parameters of the simulation are shown in Table I.

Fig. 8 shows that by controlling voltage of HF inverter in front of the DC/DC, when the vehicle battery charging power is constant, regardless of how illumination changes, HF inverter DC bus voltage 300V has remained unchanged. When a second EV is connected at 2.7s, the EV battery charging power increases, and the HF inverter DC bus voltage increases.

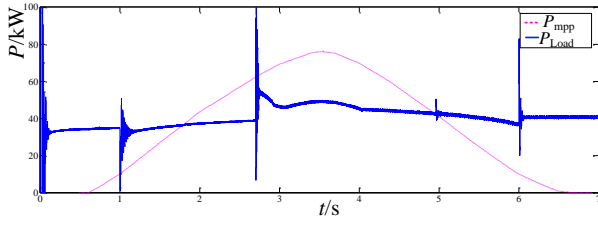
TABLE I. MAIN SIMULATION PARAMETERS

Parameters	values
Maximum power of photovoltaic generation/kW	100
Battery capacity/Ah	800
Onboard battery1capacity/Ah	100
Onboard battery2capacity/Ah	50
HF inverter operating frequency/kHz	20
Transmitting/receiving coils inductance/ $\mu$ H	300
Transmitting capacitance/nF	190
Receiving capacitance/nF	160
Transmitting/receiving coils Mutual inductance/ $\mu$ H	60

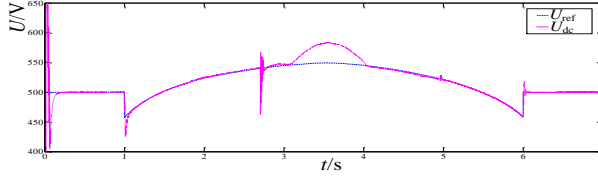
Figs. 8(a)-(e) show the simulation results of the microgrid system, including the PV power generation, the battery current and voltage, and the DC microgrid voltage levels. As can be seen from Figure 8(e), with the continuous access of the car battery the charging power will increase, and the input power of the HF inverter will increase at the same time.

Figs. 8(f) and 8(g) show that when the vehicle battery charging power changes, the transmission coil voltage/current of wireless power transmission also changes. Fig. 8(h) shows that the car battery charging power began to remain unchanged at 7.8kW. When the second EV is connected, power stabilized at about 11.8kW. From DC bus terminal of the HF inverter to the DC/DC for car battery charging energy transfer efficiency is more than 80%, including the loss of HF inverter side DC/DC converter, the DC/AC inverter, the transmitting/receiving coils, the AC/DC rectifier and the DC/DC power converter charging for the vehicle battery.

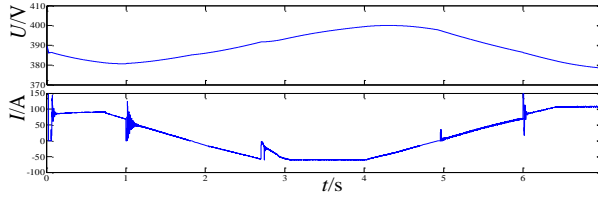




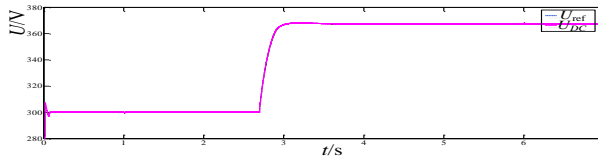
(a) Maximum PV power and load power.



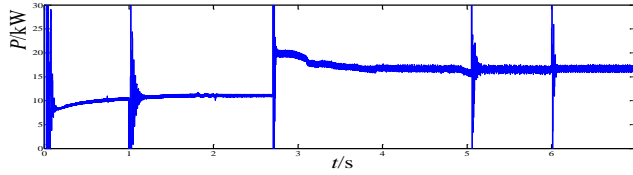
(b) Reference value and actual value of PV side DC bus voltage.



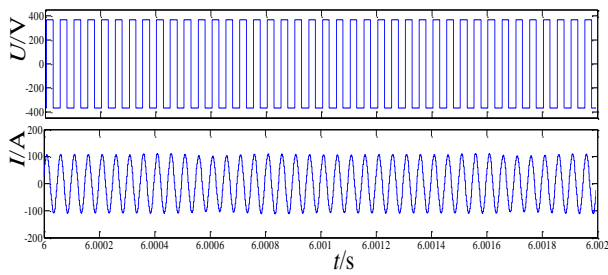
(c) Battery charging/discharging voltage and current.



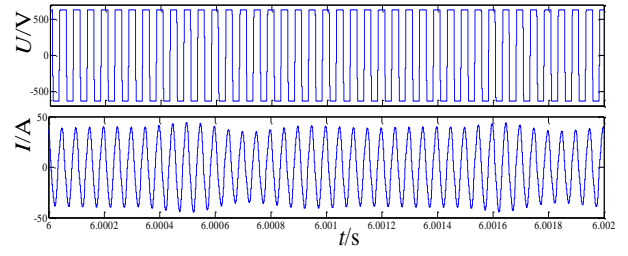
(d) Reference and actual values of DC bus voltage of HF inverter.



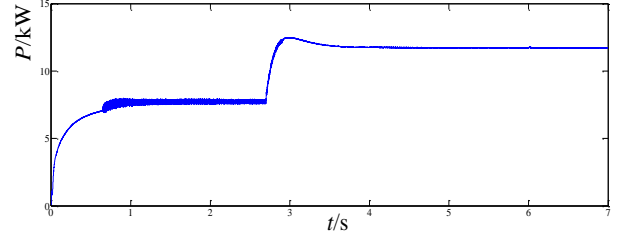
(e) Input power of HF inverter.



(f) Charging voltage/current of the transmitting coils.



(g) Voltage and current at the receiving coils.



(h) Total power of the DC bus on the battery side.

Fig. 8. Simulation results.

## VI. EXPERIMENTAL RESULTS

In order to further verify the feasibility of the system design, experimental results from the EV wireless charging station are obtained. The experimental system is shown in Fig. 9, which consists of a DC power supply, a HF inverter, the WPT of transmitting/receiving coils, the electric vehicle and its controller. The main parameters of the experimental setup are shown in Table II.

TABLE II MAIN PARAMETERS OF THE LAB SETUP

Parameters	Values
DC supply voltage/V	0-500
Primary inductance/ $\mu$ H	248
Secondary inductance/ $\mu$ H	149
working frequency/kHz	20
transmission distance/cm	20
Onboard battery capacity/Ah	100



Fig.9 Lab system of the EV wireless charging.

## REFERENCES

- [1] Chen Qingquan, Sun Liqing, "Present status and future trends of electric vehicles," *Science & Technology Review*, 2005, 23(4) : 24-28.
- [2] Xiao Xiangning, Wen Jianfeng, Tao Shun, et al., "Study and recommendations of the key issues in planning of electric vehicles' charging facilities." *Transactions of China Electrotechnical Society*, 2014, 29(8) : 1-10.
- [3] Wang Chengshan, Wu Zhen, Li Peng. Research on key technologies of microgrid. *Transactions of China Electrotechnical Society*, 2014, 29(2) : 1-12.
- [4] Yang Xinfu, Su Jian, L u Zhipeng, et al. Overview on micro-grid technology. *Proceedings of the CSEE*, 2014, 34(1) : 57-70.
- [5] Guo Li, Liu Wenjian, Jiao Bingqi, et al. Multi-objective optimal planning design method for stand-alone microgrid system. *Proceedings of the CSEE*, 2014, 34(4) : 524-536.
- [6] Castilla M, Miret J, Sosa J L, et al, "Grid-fault control scheme for three-phase photovoltaic inverters with adjustable power quality characteristics," *IEEE Trans. Power Electron.*, 2010, 25(12): 2930-2940
- [7] Xiao Xiangning, Chen Zheng, Liu Nian. Integrated mode and key issues of renewable energy sources and electric vehicles' charging and discharging facilities in microgrid . *Transactions of China Electrotechnical Society*, 2013, 28(2) : 1-14.
- [8] Van Roy J, Leemput N, Geth F, et al. Electric vehicle charging in an office building microgrid with distributed energy resources[J]. *IEEE Transactions on Sustainable Energy*, 2014.
- [9] Lopes J A P, Soares F J, Almeida P M R. Integration of electric vehicles in the electric power system. *Proceedings of the IEEE*, 2011 , 99(1) : 168-183.
- [10] Mao Meiqin, Sun Shujuan, Su Jianhui. Economic analysis of a microgrid with wind/photovoltaic/storages and electric vehicles . *Automation of Electric Power Systems*, 2011, 35(14) : 30-35.
- [11] Zhao Zhengming, Zhang Yiming, Chen Kainan. New progress of magnetically-coupled resonant wireless power transfer technology. *Proceedings of the CSEE*, 2013, 33(3) : 1-13+21.
- [12] Thrimawithana D J, Madawala U K, Neath M A., "Synchronization technique for bidirectional IPT systems," *IEEE Transactions on Industrial Electronics*, 2013, 60(1) : 318-328.
- [13] Song Xianjin, Liu Guoqiang, Zhang Chao, et al, "Resonance wireless charging technology in separate groups for the power battery packs of electric buses," *Trans. China Electrotechnical Society*, 2013, 28(2):92-98.
- [14] Cao Lingling, Chen Qianhong, Ren Xiaoyong, et al. Review of the efficient wireless power transmission technique for electric vehicles," *Transactions of China Electrotechnical Society*, 2012, 27(8) : 1-13.
- [15] XIAO Zhaoxia, LIU Jie, "System of PV-Battery Microgrid Wireless Charging for Electric Vehicles," Chinese Patent: 201410697361, 2015-4-10.
- [16] Tang Lei, Zeng Chengbi, Miao Hong, et al., "A Novel Maximum Power Point Tracking Scheme for PV Systems Under Partially Shaded Conditions Based on Monte Carlo Algorithm," *Transactions of China Electrotechnical Society*, 2015, 30(1) : 170-176

The WPT uses Litz wire winding. It consists of a plurality of thin copper wires which can effectively reduce the resistance caused by the skin effect of the HF current.

When the DC power output voltage is 320V, the coil parameters can be optimized by the corresponding tuning capacitor, the wireless power transmission system coil voltage/current waveform, and the receiver voltage/current waveform shown in Figs.10 and 11.

As shown in Figs. 10 and 11, the transmitting coil can work stable at 20kHz, and the phase difference of voltage and current is very small after the optimization of the transmitter coil and inductor. Under the action of the resonant power transmission system, the electric energy is transmitted to the receiving coil efficiently. The energy transfer efficiency of the receiving and transmitting coils reaches more than 90%.

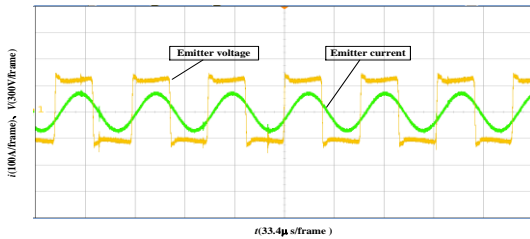


Fig. 10. Voltage and current of the transmitting coil

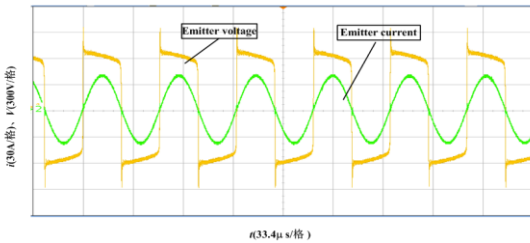


Fig. 11. Voltage and current of the receiving coil.

## VII. CONCLUSION

In this paper, the hierarchical control of a PV based microgrid with electric vehicles wireless charging station is presented. Through the analysis and comparison of simulation and experimental results, the conclusions are as follows.

A hierarchical control strategy for a PV based DC microgrid HF inverter side DC voltage controller can change the wireless charging power by regulating the DC bus voltage. A wireless charging system was designed by optimizing the inductor and compensation capacitor parameters, thus the wireless charging system is in the resonance state, so as to achieve the best transmission efficiency. The simulation and experimental results show that the transmitting/receiving coils energy transfer efficiency can reach above 90%, while the wireless charging system overall energy transfer efficiency can reach 80%.

## ACKNOWLEDGEMENT

This work was supported by the Tianjin Science and Technology Support Program Key Project and National Natural Science Foundation of China (15JCZDJC32100, 17JCZDJC31300 and 51577124).